Pacific Graphics (2018)
H. Fu, A. Ghosh, and J. Kopf (Editors)

Short Paper

Anisotropic spectral manifold wavelet descriptor for deformable shape analysis and matching

Qinsong Li[1], Shengjun Liu*[1,3], Ling Hu*[1,2] and Xinru Liu[1]

[1] Institute of Engineering Modeling and Scientific Computing, Central South University, Changsha, Hunan 410083, China
[2]School of Mathematics and Computational Science, Hunan First Normal University, Changsha, Hunan 410205, China
[3]State Key Laboratory of High Performance Manufacturing Complex, Central South University, Changsha, Hunan 410083, China

Abstract

In this paper, we present a novel framework termed Anisotropic Spectral Manifold Wavelet Transform (ASMWT) for shape analysis. ASMWT comprehensively analyzes the signals from multiple directions on local manifold regions of the shape with a series of low-pass and band-pass frequency filters in each direction. Using the ASMWT coefficients of a very simple function, we efficiently construct a localizable and discriminative multiscale point descriptor, named as the Anisotropic Spectral Manifold Wavelet Descriptor (ASMWD). Since the filters used in our descriptor are direction-sensitive and able to robustly reconstruct the signals with a finite number of scales, it makes our descriptor be intrinsic-symmetry unambiguous, compact as well as efficient. The extensive experimental results demonstrate that our method achieves significant performance than several state-of-the-art methods when applied in vertex-wise shape matching.

1. Introduction

In geometry processing, computer graphics and computer vision, shape descriptors are commonly used in extensive applications. They play an important role in the success of the applications. One prominent approach to construct shape descriptors is to define a point descriptor or signature that can capture the most notable characteristics of a given shape through encoding the neighborhood of each point. Among extensive strategies to construct such point descriptors, the most popular one is called Spectral Descriptor [SOG10, BMM*15], which is generated from the processing on the eigen-functions and eigenvalues of the Laplace-Beltrami operator (LBO). The representative works of such methods include the heat kernel signature (HKS) [SOG10] and the wave kernel signature (WKS) [ASC11]. However, the HKS suffers the problem that it is highly dominated by the information from low frequencies, while conversely a portion of such low frequency information is absent in the WKS, which easily results in matching noises. Some efforts have been put forward to improve their performance [LB14].

Recently, Hammond et al. [HVG11] developed Spectral Graph Wavelet Transform (SGWT) to perform multiresolution analysis for the signals on graphs. Actually, the filters in SGWT include both low-pass and band-pass filters, which allows to integrate the advantages of the two above spectral descriptors. Utilizing the multiple layers of SGWT coefficients, Li et al. [LH13] constructed a pyramid descriptor. However, their work mainly focuses on the shape retrieval and is not sufficient discriminative and compact for shape matching.

Another common shortcoming of the above mentioned spectral descriptors is that they are isotropic and insensitive to the direction information of the shape. Therefore, they are ambiguous under its intrinsic symmetries. As to this problem, several strategies have been exploited to incorporate the important direction information for 3D shape analysis [MBBV15, BMR*16].

Contributions In this article, we firstly propose a novel powerful tool to process and analyze the signals defined on manifolds, named as Anisotropic Spectral Manifold Wavelet Transform (ASMWT). The core idea is based on the eigen-systems of Anisotropic Laplace-Beltrami Operator (ALBO) provided in [BMR*16] to extend SGWT to be direction-aware. In this new framework, the anisotropic levels of the wavelet can be flexibly controlled, as well as their orientations by specifying different parameters. Benefitting from the desirable properties of ASMWT, we utilize only one single layer of the ASMWT coefficients of a very simple intrinsic signal on a manifold to construct a very robust, compact, computation efficient, and highly discriminative point descriptor for point-wise matching between shapes. Moreover, the descriptor is also isometric-deformation invariant and especially, unambiguous to the intrinsic symmetry. Experiment results show that it outperforms the state-of-the-art methods.

2. Anisotropic Laplace-Beltrami Operator

We model a shape as a connected smooth compact two-dimensional manifold (surface) X (possible with boundaries) embedded in $\mathbb{R}^3$. Given a Riemannian metric for this shape, $< f, g >_{L^2(X)} =$

DOI: 10.2312/pg.20181276

$\int_X f(x)g(x)dx$ expresses the standard inner product on it and the space of the square integrable real functions is denoted as $L^2(X) = \left\{ f : X \to \mathbb{R}, \int_X f(x)^2 dx < \infty \right\}$, where dx is the area element induced by this Riemannian metric. The second fundamental form, a 2×2 matrix, its eigenvalues, κ_M and κ_m, are called the principal curvatures and their corresponding eigenvectors $\mathbf{V}_M(x)$ and $\mathbf{V}_m(x)$ constitutes an orthonormal basis on the tangent plane T_xX at point x. In order to model a heat flow that is position and direction dependent, Boscaini et al [BMR*16] defined ALBO as following

$$\Delta_{\alpha\theta} f(x) = -\mathrm{div}_X(\mathbf{R}_\theta \mathbf{D}_\alpha(x) \mathbf{R}_\theta{}^T \nabla_X f(x)),$$

where $\nabla_X f$ and $\mathrm{div}_X f$ are the intrinsic gradient and the divergence of $f(x) \in L^2(X)$ respectively. $\mathbf{D}_\alpha(x) = \begin{bmatrix} \frac{1}{1+\alpha} & \\ & 1 \end{bmatrix}$ is the thermal conductivity tensor acting on the intrinsic gradient direction in the tangent plane (represented in the orthogonal basis $\mathbf{V}_M(x)$ and $\mathbf{V}_m(x)$ of principal curvature directions) and used to control the anisotropic level along the maximum curvature direction. $\mathbf{R}_\theta$ is a rotation by θ in the tangent plane, which endows ALBO with multiple anisotropies at angle θ w.r.t. the maximum curvature direction. Note that, when $\alpha = 0$, $\theta = 0$, ALBO becomes the conventional Laplace-Beltrami operator.

In practical applications, a 3D shape surface is usually discretized into a triangular mesh and the discretization of the ALBO takes the form of a sparse matrix. Given a mesh $M = (V, E, F)$, it includes N vertices $V = \{1, \cdots, N\}$, a set of edges E and a set of triangles $F = (ijk)$. For each triangle ijk, we firstly compute the directions of principal curvature $\mathbf{V}_M, \mathbf{V}_m$, then attach an orthonormal reference frame $\mathbf{U}_{ijk} = [\mathbf{V}_M, \mathbf{V}_m, \mathbf{n}] \in \mathbb{R}^{3\times 3}$ to it, where $\mathbf{n}$ is the unit normal vector to this triangle. The tensor $\mathbf{D}_\alpha$ operating on its tangent vectors is expressed w.r.t $\mathbf{U}_{ijk}$ as $\mathbf{D}_\alpha = \begin{bmatrix} \frac{1}{1+\alpha} & & \\ & 1 & \\ & & 1 \end{bmatrix}$. Let $\mathbf{e}_{ij} \in \mathbb{R}^3$ denote the oriented edge pointing from vertex i to vertex j, normalized to unit length. Define the $\mathbf{H}_\theta$-weighted inner product between edges $\mathbf{e}_{kj}$and $\mathbf{e}_{ki}$ as

$$\left\langle \mathbf{e}_{kj}, \mathbf{e}_{ki} \right\rangle_{\mathbf{H}_\theta} = \mathbf{e}_{kj}^T \underbrace{\mathbf{R}_\theta \mathbf{U}_{ijk} \mathbf{D}_\alpha \mathbf{U}_{ijk}^T \mathbf{R}_\theta^T}_{\mathbf{H}_\theta} \mathbf{e}_{ki},$$

where $\mathbf{R}_\theta$ is the corresponding 3×3 rotation matrix when rotating the basis vectors $\mathbf{U}_{ijk}$ on each triangle around the respective normal $\mathbf{n}$ by the angle θ. Now, we can get $N \times N$ ALBO matrix $\mathbf{L}_{\alpha\theta} = -\mathbf{A}^{-1}\mathbf{B}_{\alpha\theta}$. The element a_i of the mass matrix $\mathbf{A} = \mathrm{diag}(a_1, \cdots, a_N)$ denotes the local area element at vertex i and the stiffness matrix $\mathbf{B}_{\alpha\theta} = (b_{ij})$ is composed of weights

$$b_{ij} = \begin{cases} -\frac{1}{2}\left(\frac{\langle \mathbf{e}_{kj}, \mathbf{e}_{ki} \rangle_{\mathbf{H}_\theta}}{\sin \beta_{ij}} + \frac{\langle \mathbf{e}_{kj}, \mathbf{e}_{ki} \rangle_{\mathbf{H}_\theta}}{\sin \gamma_{ij}} \right), & (i,j) \in E, \\ -\sum_{k \neq i} b_{ik}, & i = j, \\ 0, & otherwise. \end{cases} \quad (1)$$

where β_{ij}, γ_{ij} are the two angles opposite to the edge between vertices i and j in the two triangles sharing the edge.

3. Anisotropic spectral manifold wavelet transform

In this section, we extend SGWT to be direction sensitive based on the eigen-decompositon of ALBO. On the triangular mesh M, a function f is represented as a N-dimensional vector $\mathbf{f}$. The inner product of two functions on the mesh f and g is discretized as $\langle \mathbf{f}, \mathbf{g} \rangle = \mathbf{f}^{\mathrm{T}} \mathbf{A} \mathbf{g}$, where $\mathbf{A}$ is the mass matrix. The eigen-decomposition of ALBO can be solved as a generalized eigenproblem $\mathbf{B}_{\alpha\theta}\phi_{\alpha\theta,k} = \lambda_{\alpha\theta,k}\mathbf{A}\phi_{\alpha\theta,k}$, where $\lambda_{\alpha\theta,k}$ is the kth eigenvalue of matrix $\mathbf{L}_{\alpha\theta}$ and $\phi_{\alpha\theta,k}$ is the corresponding eigenvector. In practice, we usually only need the first K eigenvectors and eigenvalues.

Given a wavelet kernel $g(\lambda)$ and a scaling function kernel $h(\lambda)$, which are analogous to a band-pass and low-pass filter, the Anisotropic spectral manifold wavelets (ASMW) and the scaling functions are respectively defined as

$$\psi_{\alpha\theta,tm}(n) = \sum_{k=0}^{K-1} a_m g(t\lambda_{\alpha\theta,k}) \phi_{\alpha\theta,k}(m) \phi_{\alpha\theta,k}(n),$$

$$\varphi_{\alpha\theta,m}(n) = \sum_{k=0}^{K-1} a_m h(\lambda_{\alpha\theta,k}) \phi_{\alpha\theta,k}(m) \phi_{\alpha\theta,k}(n).$$

where $m, n = 1, 2, \cdots, N$ are the indices of the vertices and m represents the location of the wavelets and the scaling functions, and t is the wavelet scale. Correspondingly, the transform coefficients are given as

$$W_f(\alpha\theta, tm) = \left\langle \mathbf{f}, \psi_{\alpha\theta,tm} \right\rangle_{\mathbf{A}} = \sum_{k=0}^{K-1} a_m g(t\lambda_{\alpha\theta,k}) \hat{f}_{\alpha\theta}(k) \phi_{\alpha\theta,k}(m)$$

$$S_f(\alpha\theta, m) = \left\langle \mathbf{f}, \varphi_{\alpha\theta,m} \right\rangle_{\mathbf{A}} = \sum_{k=0}^{K-1} a_m h(\lambda_{\alpha\theta,k}) \hat{f}_{\alpha\theta}(k) \phi_{\alpha\theta,k}(m),$$

where $\hat{f}_{\alpha\theta}(k) = \left\langle \mathbf{f}, \phi_{\alpha\theta,k} \right\rangle_{\mathbf{A}}$. In this paper, as to consider all the frequencies equally-important overall, we use Mexican-hat wavelet kernel $g(\lambda) = \lambda \exp(-\lambda)$ and the scaling function kernel $h(\lambda) = 1.2\exp\left(-\left(\frac{\lambda}{0.4\lambda_{\min}}\right)^4 - 1\right)$. For any practical computation, the continuous scale parameter t of the wavelets must be sampled to a finite number of scales. Choosing J scales $\{t_j\}_{j=1}^J$ will yield a collection of $N \times J$ wavelet functions $\psi_{\alpha\theta,t_jm}$. The minimum and maximum scales of the discretized wavelet t_J and t_1 are computed as $t_J = 1/\lambda_{\max}$, where $\lambda_{\max}$ is the upper bound of the spectrum of $\mathbf{L}_{\alpha\theta}$ and $t_1 = 2/\lambda_{\min}$, here $\lambda_{\min} = \lambda_{\max}/e_{low}$ and $e_{low} > 0$ is a user-defined parameter determining the lower bound of the spectrum. The remaining scales $t_J \leq t_j \leq t_1$ are spaced logarithmically equispaced between the minimum scales t_J and maximum scales t_1. Obviously, SGWT is the special case when $\alpha = 0, \theta = 0$. We show a series of ASMW determined by various parameters in **Figure** 1.

4. The proposed ASMW descriptor

For each vertex i of the mesh, we choose the ASMWT coefficients of the delta function δ_i to encode the multiscale local context around the point. For a given α and θ, utilizing J scales wavelet coefficients and the corresponding scaling function coefficients, we define a J+1 dimensional row vector

$$d_{\alpha\theta}(i) = \left(S_{\delta_i}(\alpha\theta, i), W_{\delta_i}(\alpha\theta, t_1 i), W_{\delta_i}(\alpha\theta, t_2 i), \cdots, W_{\delta_i}(\alpha\theta, t_J i)\right)$$

to describe the shape information at angle θ. To comprehensively capture the information from all directions around each point,

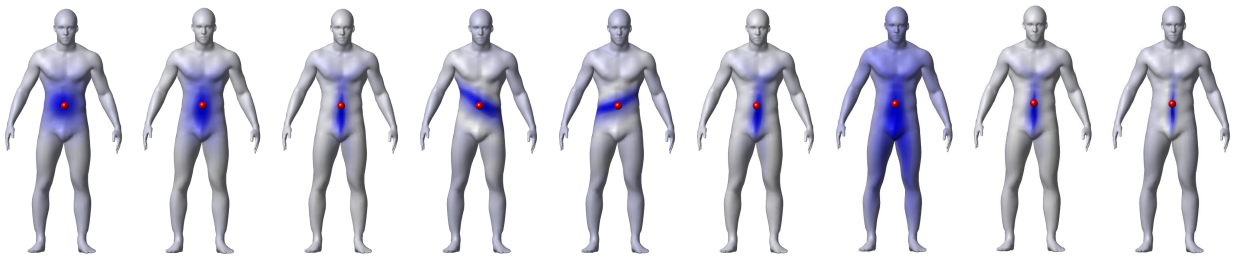

Figure 1: *ASMW determined by varied parameters. From the left to right, wavelets on the first three shapes are determined by different anisotropic levels* $\alpha = 0(isotropic), 3, 300$ *, the middle three by different angles* $\theta = \pi/4, \pi/2, 3\pi/4$ *and the right three by different scales* $t_j, j = 1, 3, 5$*. The other parameters are the same in each three ones.*

we use L equally-spaced rotation angles $\theta = \theta_1, \theta_2, \cdots, \theta_L$, $\theta \in [0, 2\pi)$. Finally, combining each $d_{\alpha\theta_l}(i)$, $l = 1, 2, \cdots, L$, we build our ASMW descriptor, a $L(J+1)$ dimensional row vector

$$\mathrm{ASMWD}(i) = (d_{\alpha\theta_1}(i), d_{\alpha\theta_2}(i), \cdots, d_{\alpha\theta_L}(i)).$$

Optionally, we may also use multiple degrees of anisotropy, α_1,α_2, . . . , α_A.

ASMWD has lots of desirable properties. It is invariant under the isometric deformations and able to distinguish the intrinsic symmetry of the shape. We show these two properties in Figure 2(a) and Figure 2(b) respectively.

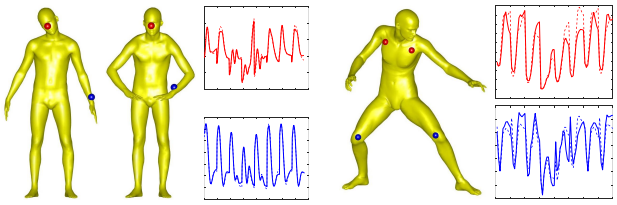

(a) (b)

Figure 2: *Illustration of the properties of ASMWD. (a) Isometric deformation invariant. The two shapes have isometric deformation between them and the solid and dotted curves represent the ASMWD of the two points(corresponding to the point with the same color) on the left and right shape respectively. (b) Disambiguity of the intrinsic symmetry. ASMWDs are computed at two pairs of intrinsic symmetric points on a human shape. Solid curves are for the descriptors of the left-part points and dotted curves are for right points.*

5. Experiments and results

In this section, we will employ our descriptor in point-to-point matching for extensive challenging shapes. All experiments are tested on a PC with Intel(R) Core i7-4790 CPU at 3.60 GHz and 16.0 GB RAM.

The public dataset CAESAR [PWH*17] is used to test the descriptor performance. CAESAR is the largest commercially available dataset that contain 3D scans of over 4500 subject in a standard pose. We select a random set of 20 shapes from the fitted-meshes subset of this dataset where each shape has nearly 6K vertices. These datasets are considerably challenging due to the presence of non-isometric deformations as well as significant variability between different human subjects. Set K = 200, J=5, L = 8 and anisotropic level $\alpha = 10$ to compute our descriptor and the code and settings of other methods in the comparison are provided online. For a fair comparison, all the dimensions of the descriptors are set to 48 if without special account. The matched point for each point is obtained using nearest neighbor search in descriptor space, where the distance between points is evaluated by Euclidean distance of the descriptors.

Quantitative evaluation We use three criteria to evaluate descriptor performance including cumulative match characteristic (CMC), receiver operator characteristic (ROC) and correspondence quality characteristic (CQC). Note that, all the above criteria were evaluated with the asymmetric setting where we consider symmetric points as incorrect matching, which is more rigorous than those commonly used in spectral analysis.

The performance comparison with several state-of-the-art descriptors is demonstrated in Figure 3. Those methods resulted from LBO are plotted by dashed curves while ALBO by solid curves. It is clearly seen that ASMWD outperforms all competitors. There exist very distinct gaps between ASMWD and the isotropic descriptors, such as HKS, WKS, WFT [BMM*15]. This means that the direction information plays important role to improve the performance of the descriptor. For completely comparison, we also make comparison with AHKS [BMR*16] and AWFT [MRCB16], both also generated from ALBO eigen-decomposition while using different filters. The results show the outstanding advantages of the filters(wavelet kernels and scaling function kernels) used in our method. Moreover, DEP [MOR*18] and AWFT have much lower computation efficiency than ASMWD, since DEP needs to solve a number of linear systems of equations and AWFT requires amount of input signals and too much transform coefficients for each signal.

Qualitative evaluation In Figure 4, we demonstrate the robust performance of our descriptor on several human models with different deformations. The results show that our descriptor manifests good localization and specificity, and disambiguate the intrinsic-symmetry even under some large deformations.

6. Conclusion and future work

In this paper, we introduced a novel framework termed anisotropic spectral manifold wavelet transform for shape analysis. The gener-

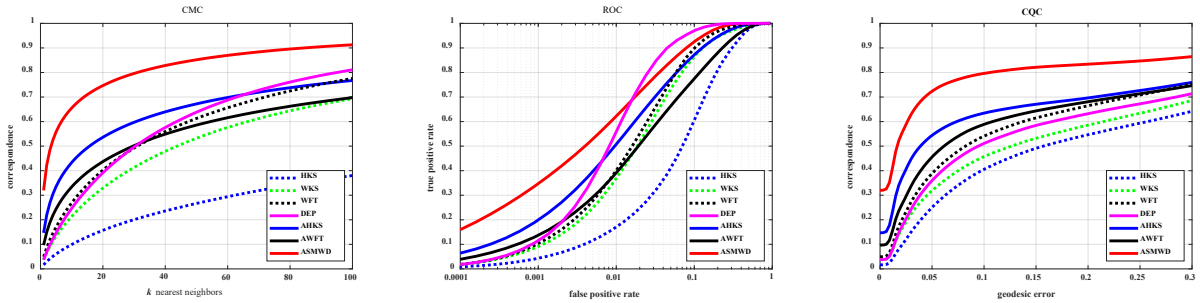

Figure 3: *The performance evaluation on CAESAR dataset. All descriptors in these plots are 48-dimensional vectors.*

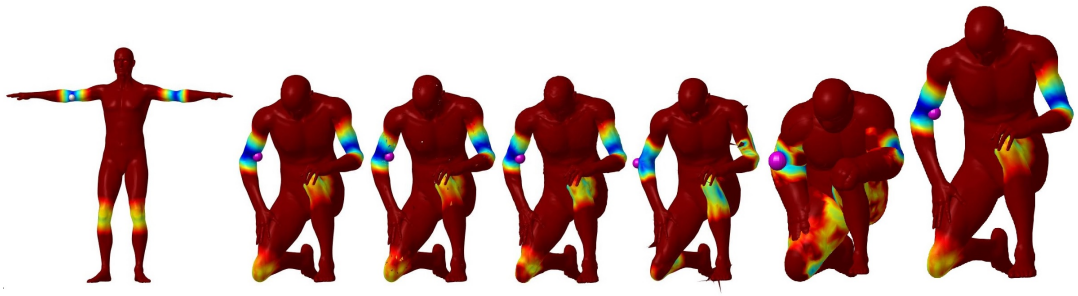

Figure 4: *The visualized Euclidean distance (Normalized) of the descriptors between a reference point(white sphere on the arm of the leftmost human shape) and the rest points on the human shapes with different transformations. From left to right the deformation the shape endured is near isometric deformation, deformation with micro holes, with noise, with sharp noise, local scaled and global scaled. The nearest point to the reference on each human shape is colored with magenta . Hotter color represents the larger distance. For visualization clarity, distances are saturated at the first* 10% *value.*

alized wavelet transform allows to capture more underlying information of the signals on manifolds from multiple directions of the local geometry of shapes. Based on the multiscale transform coefficients of a very simple function, we proposed a very discriminative and compact descriptor. We showed that our descriptors could be successfully used to address point-to-point shape matching. And extensive experiment results illustrated that it achieved significantly better performance than previous methods. In the future, other applications will be explored by using ASMWT.

7. Acknowledgements

We would acknowledge the anonymous reviewers for their valuable comments. This research is supported partially by National Natural Science Foundation of China (Grant Nos. 61572527, 61628211, 61602524).

References

[ASC11] AUBRY M., SCHLICKEWEI U., CREMERS D.: The wave kernel signature: A quantum mechanical approach to shape analysis. In *IEEE International Conference on Computer Vision Workshops* (2011), pp. 1626–1633. 1

[BMM*15] BOSCAINI D., MASCI J., MELZI S., BRONSTEIN M. M., CASTELLANI U., VANDERGHEYNST P.: Learning class-specific descriptors for deformable shapes using localized spectral convolutional networks. *symposium on geometry processing 34*, 5 (2015), 13–23. 1, 3

[BMR*16] BOSCAINI D., MASCI J., RODOLÃĂ E., BRONSTEIN M. M., CREMERS D.: Anisotropic diffusion descriptors. *Computer Graphics Forum 35*, 2 (2016), 431–441. 1, 2, 3

[HVG11] HAMMOND D. K., VANDERGHEYNST P., GRIBONVAL R.: Wavelets on graphs via spectral graph theory. *Applied & Computational Harmonic Analysis 30*, 2 (2011), 129–150. 1

[LB14] LITMAN R., BRONSTEIN A. M.: Learning spectral descriptors for deformable shape correspondence. *IEEE Transactions on Pattern Analysis & Machine Intelligence 36*, 1 (2014), 171. 1

[LH13] LI C., HAMZA A. B.: A multiresolution descriptor for deformable 3d shape retrieval. *The Visual Computer 29* (2013), 513–524. 1

[MBBV15] MASCI J., BOSCAINI D., BRONSTEIN M. M., VANDERGHEYNST P.: Geodesic convolutional neural networks on riemannian manifolds. In *IEEE International Conference on Computer Vision Workshop* (2015), pp. 832–840. 1

[MOR*18] MELZI S., OVSJANIKOV M., ROFFO G., CRISTANI M., CASTELLANI U.: Discrete time evolution process descriptor for shape analysis and matching. *Acm Transactions on Graphics 37*, 1 (2018), 1–18. 3

[MRCB16] MELZI S., RODOLA E., CASTELLANI U., BRONSTEIN M. M.: Shape analysis with anisotropic windowed fourier transform. In *International Conference on 3d Vision* (2016), pp. 470–478. 3

[PWH*17] PISHCHULIN L., WUHRER S., HELTEN T., THEOBALT C., SCHIELE B.: Building statistical shape spaces for 3d human modeling. *Pattern Recognition 67* (2017), 276–286. 3

[SOG10] SUN J., OVSJANIKOV M., GUIBAS L.: A concise and provably informative multi-scale signature based on heat diffusion. *Computer Graphics Forum 28*, 5 (2010), 1383–1392. 1